Int J Clin Exp Pathol 2014;7(7):3563-3579
www.ijcep.com /ISSN:1936-2625/IJCEP0000883

Original Article

Immune cells in primary and metastatic gastrointestinal stromal tumors (GIST)

Silke Cameron[1], Marieke Gieselmann[1], Martina Blaschke[1], Giuliano Ramadori[1], Laszlo Füzesi[2*]

[1]Clinic of Gastroenterology and Endocrinology, Georg-August University, Göttingen, Germany; [2]Institute of Pathology, Georg-August University, Göttingen, Germany. [*]Current address: Pius Hospital, Oldenburg, Germany.

Received May 25, 2014; Accepted June 9, 2014; Epub June 15, 2014; Published July 1, 2014

Abstract: We have previously described immune cells in untreated primary gastrointestinal stromal tumors (GIST). Here we compare immune cells in metastatic and primary GIST, and describe their chemoattractants. For this purpose, tissue microarrays from 196 patients, 188 primary and 51 metastasized GIST were constructed for paraffin staining. Quantitative analysis was performed for cells of macrophage lineage (Ki-M1P, CD68), T-cells (CD3, CD56) and B-cells (CD20). Chemokine gene-expression was evaluated by real-time RT-PCR. Immuno-localisation was verified by immunofluorescence. Ki-M1P+ cells were the predominant immune cells in both primary and metastatic GIST (2 8.8% ± 7.1, vs. 26.7% ± 6.3). CD68+ macrophages were significantly fewer, with no significant difference between primary GIST (3.6% ± 2.1) and metastases (4.6% ± 1.5). CD3+ T-cells were the most dominant lymphocytes with a significant increase in metastases (7.3% ± 2.3 vs. 2.2% ± 1.8 in primary GIST, $P < 0.01$). The percentage of CD56+ NK-cells was 1.1% ± 0.9 in the primary, and 2.4 ± 0.7 ($P < 0.05$) in the metastases. The number of CD20+ B-cells was generally low with 0.6% ± 0.7 in the primary and 1.8% ± 0.3 ($P < 0.05$) in the metastases. Analysis of the metastases showed significantly more Ki-M1P+ cells in peritoneal metastases (31.8% ± 7.4 vs. 18.2% ± 3.7, $P < 0.01$), whilst CD3+ T-cells were more common in liver metastases (11.7% ± 1.8 vs. 4.4% ± 2.6, $P < 0.01$). The highest transcript expression was seen for monocyte chemotactic protein 1 (MCP1/CCL2), macrophage inflammatory protein 1α (MIP-1α/CCL3) and the pro-angiogenic growth-related oncoprotein 1 (Gro-α/CXCL-1). Whilst the ligands were predominantly expressed in tumor cells, their receptors were mostly present in immune cells. This locally specific microenvironment might influence neoplastic progression of GIST at the different metastatic sites.

Keywords: Gastrointestinal stromal tumor (GIST), immune cells, microenvironment, liver metastasis, peritoneal metastasis

Introduction

Gastrointestinal stromal tumors (GIST) are rather rare, however they are the most common soft tissue tumors of the gastrointestinal tract with an incidence of approximately 15 per million per year [1].

GIST are believed to develop from the interstitial cells of Cajal, pacemaker cells of the gut or their precursor cells, and thus generally immunohistochemically stain for c-KIT (CD117 antigen). Oncogenic mutations in receptor tyrosine kinases lead to the activation of cell-signalling cascades involved in the regulation of cell proliferation, chemotaxis and adhesion [2]. GIST can occur at any location within the gastrointestinal tract. GIST of the stomach are the most common (about 60 %), followed by the small intestine (25-35%), and colon (5%) [3-5]. They occur at a median age of 55-65 years, without gender predilection [3]. Lymph node metastasis is negligible. Distant metastatic spread mainly involves the liver and the peritoneal cavity [6]. GIST have been included into the UICC/TNM classification of malignant tumors [7] considering tumor size and mitotic activity. The classification follows the criteria for risk of recurrence established by Fletcher et al. [8]. To predict the malignant potential of GIST at the different locations, the classification by Miettinen, et al. (AFIP-criteria) additionally integrates primary tumor location in view of size and mitotic activity [5]. The cytological morphology (spindle, epithelioid or mixed) seems to have some prognostic value [9, 10]. Furthermore, it has been

Table 1. Composition of the study collective

No. of patients	196	
Age (years)	Median	Range
Primary operation	67	(33-90)
Liver metastasis	64	(39-85)
Peritoneal metastasis	70	(40-81)
Sex	No. of patients	%
Male	103	52.5%
Female	88	45.0%
Unkown	5	2.5%
Tumor origin: 188 primary GIST		
Stomach	113	60.1%
Small intestine	55	29.2%
Large intestine	15	8.0%
Unkown	5	2.7%
Sites of metastases: 51 GIST metastases		
Liver	22	42.3%
Peritoneum	29	57.7%
Number of metastatic sites		
1	34 (liver 20, peritoneum 14)	66.7%
2	5 (liver 1, peritoneum 4)	9.8%
≥ 3	2 (liver 0, peritoneum 2)	3.9%

hypothesized that GIST need additional stimuli to the underlying activating mutation in the tyrosine kinase receptor, to evolve into clinical GIST [11]. As in other tumors, a tumor microenvironment can be assumed essential for tumor growth and neovascularization [12-14]. The growing tumor regulates and maintains its microenvironment by secreting chemotactic cytokines [15-17]. We and others could show, that GIST has a varying immune cell infiltrate [18-22].

Reviewing the literature, the overall impression is that whilst untreated epithelial tumors seem to have a rather inflammatory immune cell infiltrate [16, 17, 23, 24] and often originate in a pro-inflammatory setting [25-27], other (non-epithelial) tumors such as melanoma [28, 29] or GIST [19] supposedly contain non-activated immune cells such as immature dendritic cells and tumor associated macrophages (TAMs). Instead of promoting inflammation, TAMs seem to be better adapted for scavenging debris, promoting angiogenesis, and tissue remodelling [19, 30, 31]. Their lack of producing inflammatory cytokines such as Il-6 and TNF-α, as reported in our previous study [19], points to a possible "symbiotic relationship" between the tumor and local immune cells. Recent studies show, that maturation of dendritic cells and activation of macrophages and as a consequence, stimulation of the immune response can restore antitumor cytotoxic T-cell responses [18, 22, 32-36] and tumor lysis by NK-cells [36]. Even though the presence of immune cells within GIST has been described [18-22], only preliminary data are available on the differences between primary tumor and metastases in an untreated patient collective [21, 22]. Furthermore, no data are available on the expression of chemotactic cytokines in GIST.

The aim of our study was thus to analyse the frequency of immune cells necessary for tumor-host interactions, i.e. macrophages and lymphocytes, in primary GIST compared to GIST metastases at their most common sites, liver and peritoneum. For this purpose, the following immune-cell markers were chosen: Ki-M1P, as mononuclear phagocyte antigen, is a marker for rather immature macrophages, including tissue macrophages and subpopulations of immature dendritic cells [37, 38]. CD68 is a marker for macrophages, reacting with lysosomal antigens [39]. CD3 was used as a general marker for T-lymphocytes, CD56 for NK-cells, and CD20 was used as a marker for B-lymphocytes. As immune cells are recruited by the tumor, we investigated the expression of the main chemotactic and pro-angiogenic cytokines in our primary tumor collective. Monocyte chemotactic protein 1 (CCL2/MCP1) plays a central role in monocyte recruitment and transmigration [40-42]. Growth-related oncoprotein 1 (CXCL1/Gro-α) is known as pro-angiogenic factor, associated with metastatic potential [43-45]. We further investigated macrophage inflammatory protein (MIP) 1α (CCL3), 1β (CCL4), 3α (CCL20) and 3β (CCL19), which play a role in monocyte recruitment, dendritic cell migration and chemotaxis of NK-cells [46-

Table 2A. Antibodies used for immunohistochemistry

Antibody	Dilution	Pretreatment Antigen retrieval (Citrate)	Vendor (Cat.No.)
c-KIT (CD117)	1:200	heat	DAKO (A4502)
MIB1 (ki67 clone MIB1)	1:200	heat	DAKO (M7240
Ki-M1P	1:6000	protease (Sigma)	Pathology, Kiel[1] [38]
CD 68 (clone KP1)	1:6000	heat	DAKO (M0814)
CD3 (polyclonal)	1:100	heat	DAKO (A0452)
CD20cy (clone L26)	1:200	heat	DAKO (M0755)
CD56 (clone 123C3)	1:100	heat	Zymed (18-0152)

[1]commercially not available.

Table 2B. Antibodies used for immunofluorescence

Antibody	Dilution	Vendor (Cat.No.)
CCL2 (MCP-1)	1:100	R and D systems (AF-279-NA)
CCR2	1:100	Abcam (ab13310)
CXCL1 (Gro-α)	1:100	R and D systems (AF515NA)
CXCR2	1:100	Abcam (ab14935)

48]. Gro-β (CXCL2) and Gro-γ (CXCL3) are growth-related oncoproteins and play a role in mixed leukocyte recruitment. Il-8 (CXCL8) has pro-angiogenic properties [12].

Material and methods

The samples were retrieved from a consecutive series of surgically resected GIST obtained throughout the years 1991-2009, archived in the Institute of Pathology of the Medical University, Göttingen, including 188 primary and 51 metastasized GIST (22 liver and 29 peritoneal metastases) from a total of 196 patients with untreated GIST. Some patients had been re-operated for GIST recurrence (**Table 1**). Additionally, 40 snap frozen samples (34 primary tumors and 6 metastases) from an earlier series [19] were available for immunofluorescent staining and real-time PCR analysis. The analysed patients had not received imatinib or other tyrosine kinase inhibitors prior to the operation. Evaluation of malignancy was performed according to Miettinen et al. [49] and risk of aggressive behaviour was estimated according to Fletcher et al. [8]. Ethics approval for this study was obtained from the local ethics committee.

Tissue microarray and immunohistochemistry

For immunohistochemical analysis, tissue microarrays (TMA) were constructed from paraffin-embedded tumor blocks using a semi-automated manual tissue arrayer (Alphametrix GmbH, Rodgau, Germany). In each case, 3 to 6 tissue punches (mean: 4.8) each with a diameter of 1 mm have been taken from different tumor areas. Immunohistochemistry was performed using the alkaline phosphatase-method on formalin-fixed and paraffin-embedded tissue sections as described earlier [19]. Visualization of the specific primary antibody was performed using the Dako ChemMate™ Detection Kit (K5005, DAKO, Glostrup, Denmark) with NeoFuchsin as a chromogen, according to the manufacturers' instructions. Hemalaun was used as counterstain. As a negative control, non-immune serum was used. The optimal working dilutions of the antibodies are listed in **Table 2A**.

For GIST diagnosis, anti-human c-KIT antibody was used. The proliferation index was quantified using the Ki67 antigen (MIB1) from the areas with the highest mitotic activity. The following antibodies were used to characterize the immune cells within the tumor microenvironment. Ki-M1P is a fibrohistiocytic marker to detect tissue macrophages [38] and a population of CD1a negative dendritic cells (DCs) [37]. CD68 was used as a general marker for mature macrophages [39]. CD3 [50] and CD20 [51] were used to differentiate between T- and B-cells, respectively. Furthermore, CD56, a surface marker of natural killer (NK) T-cells was used [52, 53].

Evaluation of immunohistochemical stainings

Computer-guided analysis was performed for immune cells of the macrophage lineage (Ki-M1P, CD68) and lymphocytic origin (CD3, CD20, CD 56). From each tissue punch, a digital photo (at 200× original magnification; light microscope, Carl Zeiss, Jena, Germany) was taken, and a self-written computer program was used to count the immunopositive cells

Table 3. Sequences of gene-specific primers used for quantitative RT-PCR analysis

Gene		Primer sequence	Product size (bp)
CCL2 (MCP-1)	Sense:	5'-CAG CAG CAA GTG TCC CAA AG	51 bp
	Antisense:	5'-TTG GCC ACA ATG GTC TTG AA	
CCL3 (MIP-3α)	Sense:	5'-TGG TGA CAA CCG AGT GGC T	83 bp
	Antisense:	5'-TGG TGC CAT GAC TGC CTA CA	
CCL4 (MIP-1β)	Sense:	5'-CTC TCA GCA CCA ATG GGC TC	84 bp
	Antisense:	5'-GTA AGA AAA GCA GCA GGC GG	
CCL20 (MIP-3α)	Sense:	5'-GAG TTT GCT CCT GGC TGC TTT	63 bp
	Antisense:	5'-GCC GCA GAG GTG GAG TAG C	
CCL19 (MIP-3β)	Sense:	5'-GGT GCC TGC TGT AGT GTT CA	200 bp
	Antisense:	5'-GGT CCT TCC TTC TGG TCC TC	
CXCL1 (Gro-α)	Sense:	5'-GTG TGA ACG TGA AGT CCC CC	51 bp
	Antisense:	5'-GCT ATG ACT TCG GTT TGG GC	
CXCL2 (Gro-β)	Sense:	5'-CCC AAA CCG AAG TCA TAG CC	50 bp
	Antisense:	5'-TGA GAC AAG CTT TCT GCC CA	
CXCL3 (Gro-γ)	Sense:	5'-TGT GAA TGT AAG GTC CCC CG	50 bp
	Antisense:	5'-GCT ATG ACT TCG GTT TGG GC	
CXCL8 (IL-8)	Sense:	5'-ATG ACT TCC AAG CTG GCC G	53 bp
	Antisense:	5'-GCT GCA GAA ATC AGG AAG GC	
β-actin	Sense:	5'-CTG GCA CCC AGC ACA ATG	68 bp
	Antisense:	5'-CCG ATC CAC ACG GAG TAC TTG	

and the counterstained nuclei [19, 54]. A minimum of 3 representative and good quality photographs were then used for further analysis. The correctness of the obtained numbers was validated visually.

Quantitative realtime RT-PCR of chemokine transcripts

RNA was extracted from 40 (previously untreated) snap-frozen tissue samples, according to the trizol-method described previously [55]. Reverse transcription was done using the moloney murine leukaemia virus (MMLV) reverse transcriptase (Invitrogen, Darmstadt, Germany). **Table 3** shows a list of the primers, which have been gene specifically synthesized (Invitrogen, Darmstadt, Germany). Realtime RT-PCR was performed in 40 cases (34 primary GIST and 6 metastases: 3 peritoneum, 2 liver, 1 other) with the ABI Prism 7900 real-time PCR Cycler (Applied Biosystems, Foster City, CA, USA). Quantification of the mRNA was performed by relative quantification using Sybr Green UDG master mix from Invitrogen (Darmstadt, Germany). PCR conditions were set as follows: 50 °C for two minutes, 95 °C for two minutes, and 45 cycles of 95 °C/15 sec and 60 °C/30 sec. As housekeeping gene, beta-actin was used, which was checked for stability. For relative quantification of mRNA, the following arithmetic formula was used: expression of chemokine relative to β-actin = $2^{-\Delta CT}$ where ΔCT = (CT of target-CT of β-actin) [56]. For better visualization within the figures, the results were multiplied with 1000.

Immunofluorescent staining of selected chemokines and their receptors

Immunofluorescent staining (IF) was performed on kryosections (4-5 µm) of 40 fresh frozen tumor samples. Two relevant chemokines CCL2 (MCP-1) and CXCL1 (Gro-α) and their receptors were selected. For comparison of immunopositivity, anti-cKIT was used as a marker for tumor cells. Anti-CCL2 and its receptor CCR2 as well as anti-CXCL1 and its receptor CXCR2 were used as primary antibodies (**Table 2B**). The required secondary antibodies were all obtained from Invitrogen (Darmstadt, Germany). Antigens of the chemokines were visualized with anti-mouse alexa 488 (green) and of the receptors with anti-rabbit alexa 555 (red) (Molecular Probes, Invitrogen, Darmstadt, Germany). Cell nuclear counterstaining was done with 4', 6-diamidino-2-phenylindole (DAPI; Molecular Probes, Invitrogen, Darmstadt, Germany). The IF-stainings were analyzed with an epifluorescent microscope (Axiovert 200M; Zeiss, Jena, Germany). The photomicrographs were obtained using the Axiovision 4.5 software (Zeiss, Jena, Germany).

Statistical analysis

Values for the count of immune cells are expressed as means ± SD (standard deviation). Significant differences between the means were evaluated using ANOVA followed by Student's t-test. Differences of $P < 0.05$ were considered to be statistically significant. The

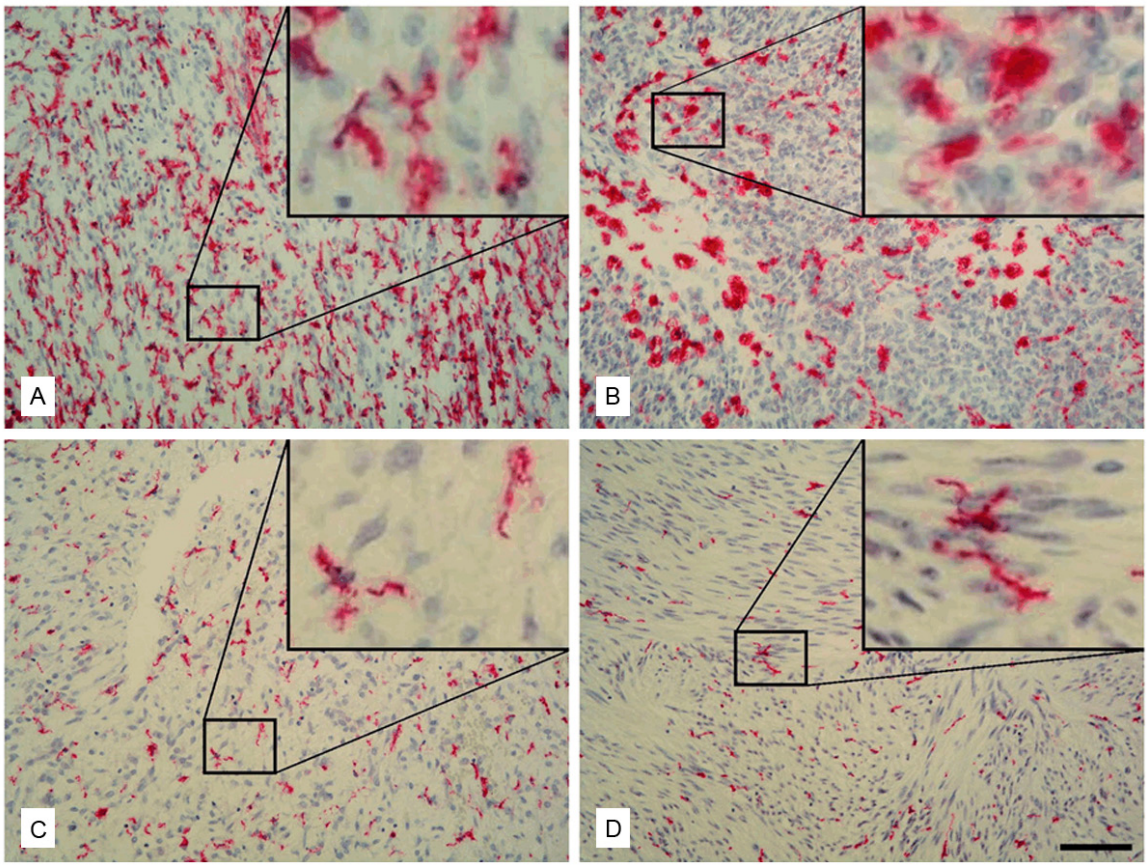

Figure 1. Representative paraffin sections showing the varying histomorphology of Ki-M1P+ cells. (A) Abundant cellular infiltrate of Ki-M1P+ fibrohistiocytes. Note their partly interdigitating dendritic projections. (B) In regressive tumor areas, Ki-M1P+ cells showed round morphology, similar to activated macrophages. In (C and D) they showed the rather delicate appearance with tender projections and spikes of dendritic cells. (Scale bar 100 µm, original magnification ×200, inlays with 4× magnification).

summary of the PCR-data is shown as box-and-whisker plot. These data were analysed using the Mann-Whitney-U-test between two unpaired groups, with $P < 0.05$ considered to be significant.

Results

Patient cohort

Tumor samples of 196 different patients were included into the analysis. 45% were female and 52.5% male (**Table 1**). The mean age at the time of operation was 68 (± 12.0) years. Women had a mean age of 66.4 years (± 13.1), whilst the age of men was about two years younger with 64.4 years (± 12.0) (**Table 1**).

Tumor location

Of the 188 primary GIST, 60.1% were located in the stomach, 29.2% in the small intestine and 8% in the colon. As for the 51 metastases, 43.1% were liver metastases, 56.8% peritoneal metastases (**Table 1**). Five of these were located retroperitoneally, however, they were attributed to the group of peritoneal metastases.

Histopathologic findings

Of the 188 primary GIST, 97.7% were c-KIT positive (CD117). 57.4% were of spindle cell morphology, 13.3% of epithelioid and 29.2% of mixed phenotype. As for the 51 metastases, 55% showed a spindle-cell phenotype, 15.7% were epithelioid, and 27.4% were of mixed cytomorphology. 1 liver metastasis could not be evaluated (1.9%). Of the 22 liver metastases, 68.2% were of spindle-cell morphology (15/22), 22.7% were of epitheloid morphology (5/22), and mixed morphology was described in 4.5% of the cases (1/22). Of the 29 peritoneal metastases 44.8% (13/29) showed spindle-cell mor-

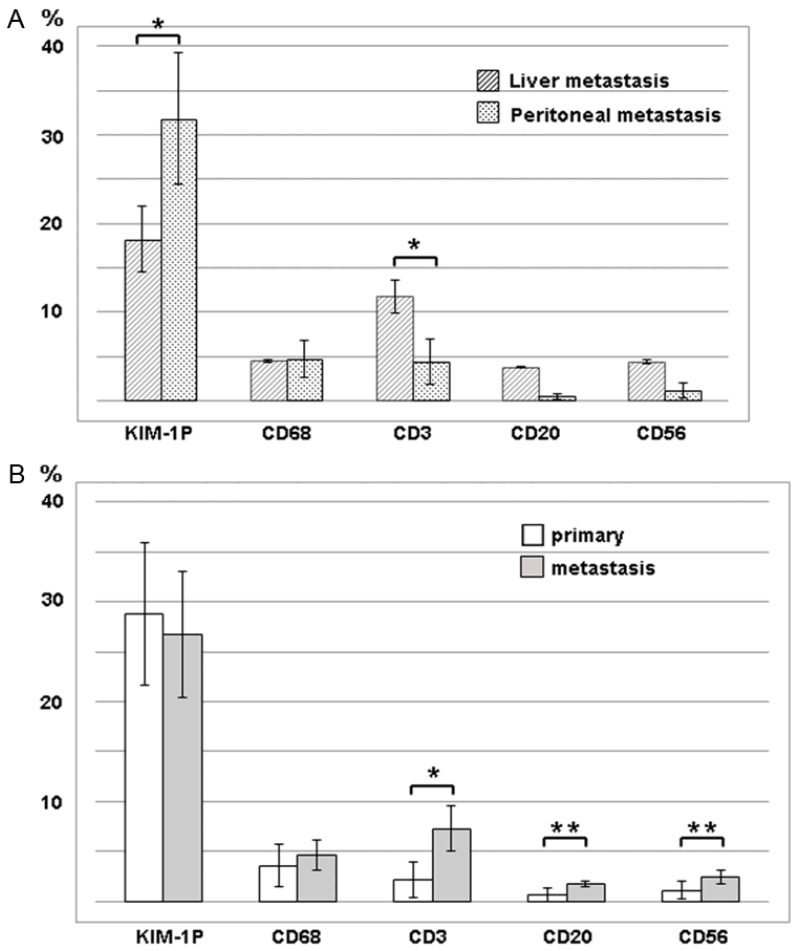

Figure 2. A: Histogram of the percentage of the different immune cells. Comparison of liver and peritoneal GIST metastases (*P < 0.01). B: Histogram of the percentage of the different immune cells. Comparison of primary and metastatic GIST (*P < 0.01; **P < 0.05).

phology and 10.3% (3/29) showed epithelioid morphology. Mixed morphology was observed in the remaining 44.8 % cases.

Association of tumor size and proliferation index

Primary GIST smaller than 5 cm in diameter had a significantly lower proliferation index than GIST larger than 10 cm (6.8% ± 8.3 versus 12.9% ± 10.8, respectively; P < 0.05). GIST of the stomach had a proliferation index of 6.1% ± 7, GIST of the small intestine of 8.3% ± 8.7 and colonic GIST of 11.7% ± 11.3. In our collective, very low and low risk GIST had a proliferation index of 3.1% ± 1.5-2.0, intermediate risk GIST had a significantly higher proliferation index of 4.9% ± 3.9 (P < 0.01) and high risk GIST had a proliferation index of 14.2% ± 10.6 (P < 0.01). Metastatic GIST had a slightly higher proliferation index of 16.1% ± 8.2 (n. s.). Interestingly, GIST located in the peritoneum had a significantly higher proliferation index (18.3% ± 7.3) compared to liver (12.9% ± 8.2; P < 0.05).

Immunohistochemical characterization of immune cells

As described earlier [19], immune cells were scattered between the tumor cells and along tumor cell bundles. However, focal accumulation of lymphocytes was also observed.

Ki-M1P+ as the most common immune cells in GIST showed a varying appearance as rather delicate cells with tender spikes and projections or as more prominent cells with dendrites, partly interdigitating. In regressive tumor areas, they showed round morphology, similar to activated (lysosomal rich) macrophages (**Figure 1**). The percentage of Ki-M1P+ cells was comparable not only at the different primary tumor sites (stomach 28.7% (± 11.4), small intestine 28.6% (± 11.8), colon 30.4% (± 12)) with a mean of 28.8% (± 7.1) but also in the metastases (26.7% ± y.6.3). Nevertheless, Ki-M1P+ cells were significantly more common in peritoneal metastases with 31.8% (± 7.4) than in the liver metastases with 18.2% (± 3.7) (P < 0.01) (**Figure 2A**).

CD68+ cells varied from round cells to cells with dendritic-cell (DC)-like appearance. CD68+ macrophages were significantly fewer than Ki-M1P+ immunohistiocytes (P < 0.01), and there was no significant difference between primary GIST (3.6% ± 2.1) and metastases (4.6% ± 1.5), neither for peritoneal nor liver metastasis (4.7 ± 2.1% vs. 4.5 ± 0.2%, respectively) (**Figures 2** and **3**).

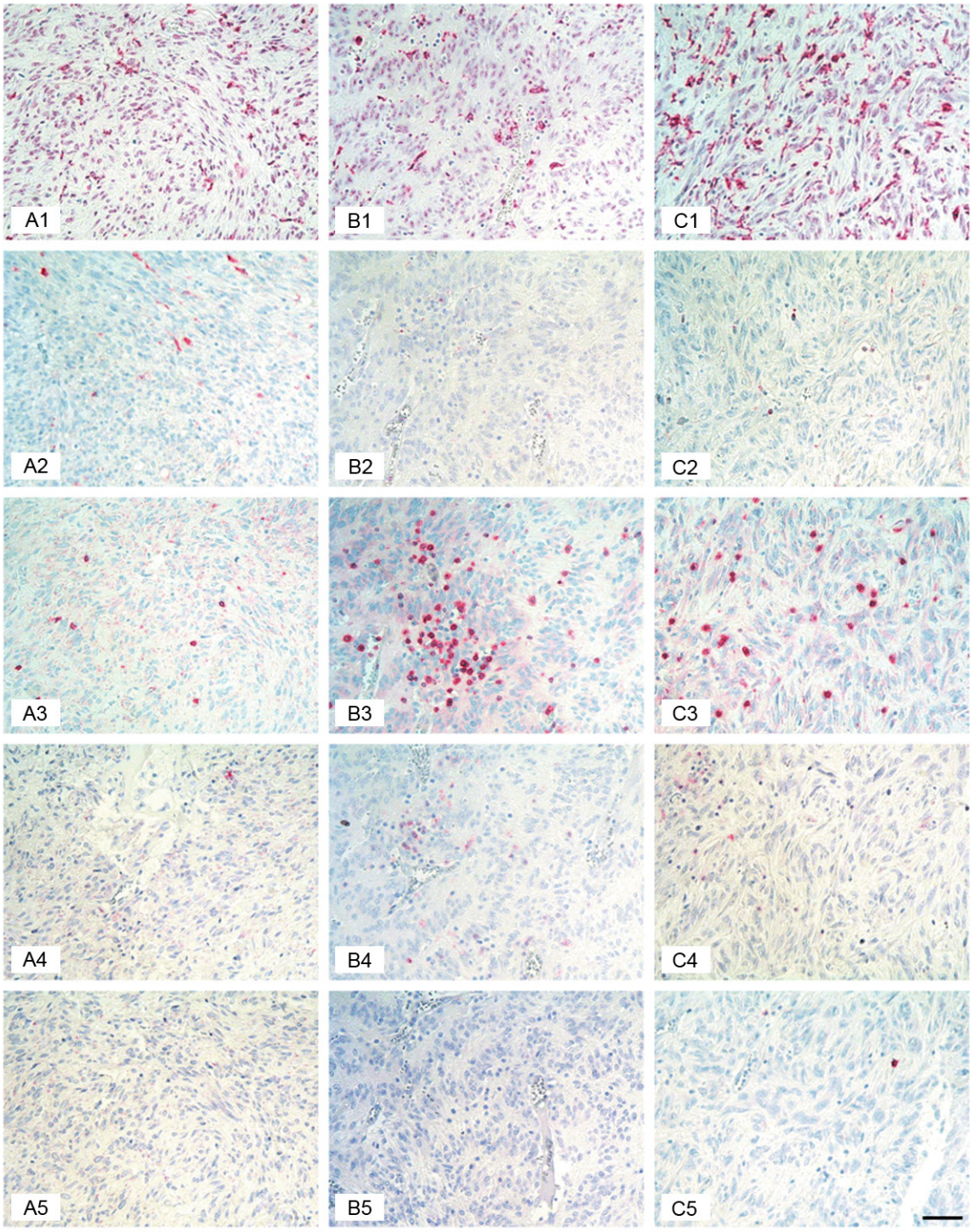

Figure 3. Representative, consecutive paraffin sections depicting the distribution of the different immune cells in a primary GIST (A), a liver metastasis (B) and a peritoneal metastasis (C). The horizontal photographs show staining with anti-Ki-M1P (1), CD68 (2), CD3 (3), CD56 (4) and CD20 (5). Counterstaining was done with hemalaun. Scale bar 100 µm, original magnification ×200.

CD3+ cells were the most abundant lymphocytes in the primary tumors (**Figures 2B** and **3**). The number of CD3+ cells in the stomach was with 1.3% ± 2.1 significantly lower than in the small intestine with 3.7% ± 5.4 ($P < 0.01$) or in the colon with 3.5% (± 6.5), ($P < 0.05$).

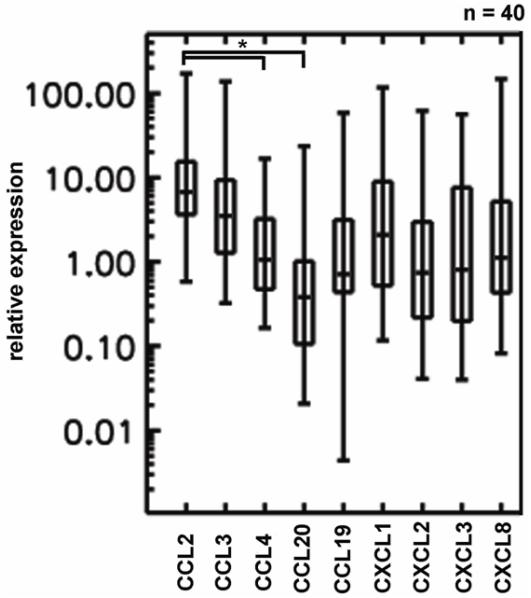

Figure 4. Relative mRNA-expression for the different chemokines. Data are shown as box-and-whisker plot on a logarithmic scale. The vertical axis depicts the expression of the target gene relative to β-actin ($\times 10^3$). The median expression is marked with a horizontal line.

Interestingly, the metastases showed significantly more CD3+ cells than the primary GIST (7.3% ± 2.3 versus 2.2% ± 1.8, respectively, $P < 0.01$) (**Figure 2B**). This can be attributed to a significantly higher number of CD3+ cells within the liver compared to peritoneal metastasis (11.7% ± 1.8 vs. 4% ± 2.6, $P < 0.01$) (**Figures 2A** and **3**).

As for the other T-cells studied, CD56+ NK-cells were more common in the metastases 2.4% ± 0.7, compared to the primaries 1.1% ± 0.9 ($P < 0.05$) (**Figure 2B**). Similar to the other T-cell markers, this increase was due to the increased number of CD56+ cells in liver metastases with 4.4% ± 0.2 in comparison to 1.1% ± 0.9 in the peritoneal metastases. No significant differences for CD56+ cells were found within primary GIST.

The number of CD20+ B-lymphocytes was generally low with 0.6% ± 0.7 in the primary and 1.8% ± 0.3 ($P < 0.05$) in the metastases (**Figure 2B**). The percentage of CD20+ cells in the stomach was 0.7% ± 2.0, and in the small intestine 0.6% ± 1.0. The slight increase in CD20+ cells in the metastases might again be attributed to the increased number of CD20+ B-cells within the liver in comparison to peritoneal metastases (3.8% ± 0.1 versus 0.4% ± 0.2, respectively). Because of the small numbers, no significance was reached.

Association of immune cells with tumor histomorphology

A strong association for the percentage of Ki-M1P+ cells with tumor morphology was found. Ki-M1P+ cells were significantly more common in epithelioid (32.1% ± 13.0) and mixed (31.7% ± 11.1), than in spindle-cellular GIST (25.8% ± 10.8; $P < 0.01$). Similar to Ki-M1P, CD68+ cells were increased in epithelioid (5.9% ± 6.7) and mixed (4.4% ± 4.2) compared to spindle-cellular GIST (3.0% ± 4.1, $P < 0.05$). For CD3+ and CD56+ cells, no such association was found.

Associations of immune cells with tumor size and proliferation index

GIST smaller than 5 cm ($P < 0.05$) showed a significantly lower number in Ki-M1P+ cells than that of GIST larger than 10 cm (27.1% ± 10.5 versus 31.85 ± 9.1). Neither for CD68, nor CD3 or CD56, a significant difference with increasing tumor size, was found.

Additionally, GIST with a proliferation index > 10% had significantly more Ki-M1P+ cells compared to GIST with a proliferation index < 10% (31.2 ± 11.1 vs. 27.5 ± 11.9; $P < 0.05$). For CD68, no significance was observed when the proliferation indices were correlated.

As for CD3+ cells, their percentage increased significantly with a proliferation index > 10% compared to GIST with a proliferation index < 10% (5.8% ± 7.6 vs. 2.3% ± 4.9, respectively; $P < 0.01$). No differences were found for CD56 cells in view of the proliferation index.

The mean percentage of CD20+ cells increased with an elevated proliferation rate > 10% (1.7% ± 5.6 versus 0.6% ± 1.3, $P < 0.05$).

Association of immune cells and risk of recurrence (according to Fletcher et al. [8])

Regardless of the location of the primary GIST, our results showed no association for Ki-M1P+ cells and risk of recurrence. For CD3+ T-cells, we found a significant increase in metastatic GIST (8.1% ± 9.4) compared to very low risk

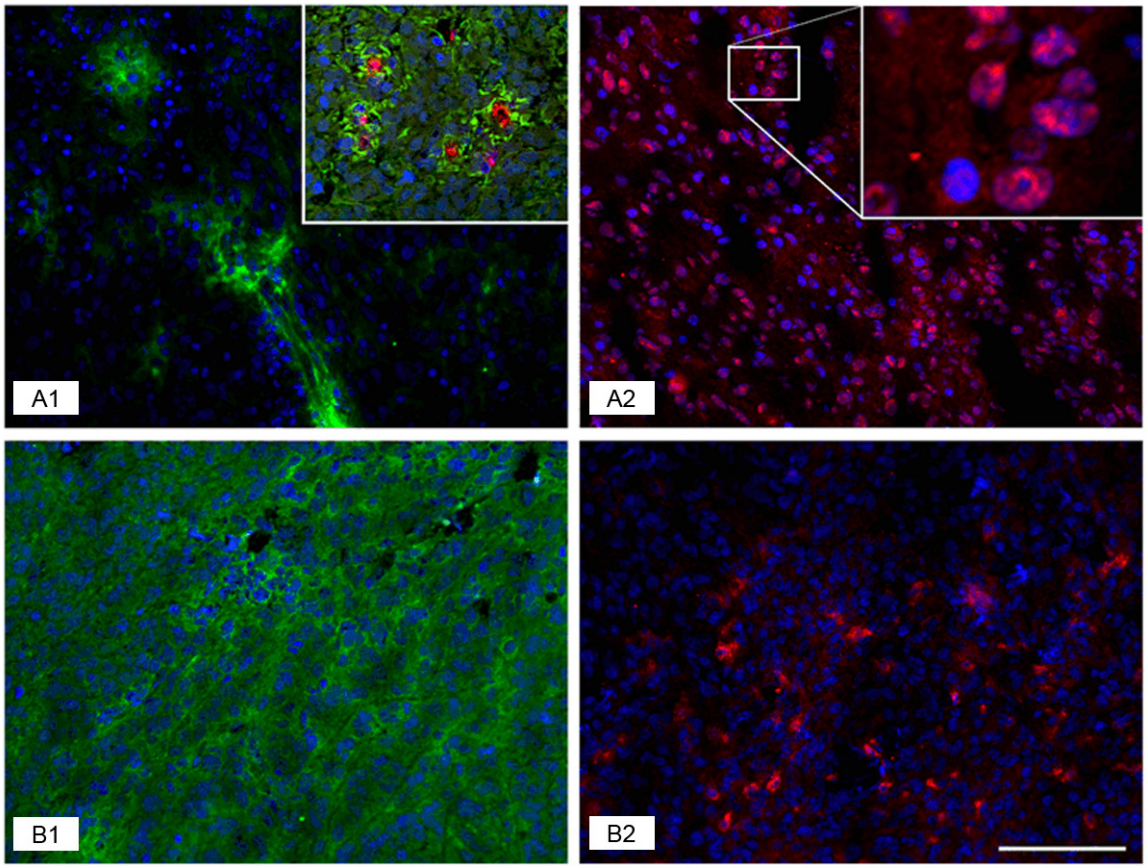

Figure 5. Immunofluorescent staining of kryosections of representative GIST. The photographs show immunostaining with anti-CCL2 (green) (1), and its receptor CCR2 (red) (2). (A) peritoneal metastasis; the inlay (A1) shows a liver metastasis (as double staining); the inlay (A2) shows a 4× magnification of the indicated area. (B) colon GIST. CCL2 shows positivity in vessels and tumor cells. Note that CCR2 can be visualized within the nuclei of the tumor cells (A2), but also tumor-infiltrating immune cells (B2). The staining pattern for both, chemokine and receptor, was independent of the tumor location. Cell nuclear counterstaining was done with 4',-6-diamidino-2-phenylindole, visualized in blue. Scale bar 100 µm, original magnification ×200.

(1.1% ± 1.8), low risk (1.5% ± 2.5), intermediate (1.9% ± 3.4) and high risk (3.7% ± 5.8) GIST ($P < 0.05$). A similar correlation was obtained for the percentage of CD56+ cells in very low (1.3% ± 1.9) and low risk (0.6% ± 0.8) but not in high risk GIST compared to metastatic (2.8% ± 6.5) GIST ($P < 0.05$). The other immune cells did not increase significantly with the GIST classification of risk for recurrence.

RNA expression of chemokines

The transcript expression of CCL2 (MCP-1), a known chemoattractant for monocyte recruitment, was highest, with a mean cycle threshold value (CT) of 26.1 ± 1.3 (**Figure 4**). The second highest expression was found for CCL3 (MIP-1α), with a mean CT value of 26.8 ± 1.6. The third highest expression was found for CXCL1 (Gro-α) with a mean CT value of 27.3 ± 1.8. IL-8 transcript expression showed a CT-value of 28.4 ± 2.1. CCL2 transcript levels were significantly higher than for CCL4 (28.9 ± 1.7) and CCL20 (MIP3α, 30.3 ± 1.6) ($P < 0.01$). CCL4 transcript expression was followed by that of CXCL3 (Gro-γ), CXCL2 (Gro-β) and CCL19 (MIP-3β). No significant differences in the expression of these chemokines in terms of tumor location or size were found.

Immunofluorescent staining of CCL2 (MCP-1) and CXCL1 (Gro-α) and their receptors CCR2 and CXCR2

CCL2 showed expression within the tumor cells, and in part by tumor vessels. Its receptor CCR2 was expressed in some tumor-infiltrating immune cells, but could mostly be visualized

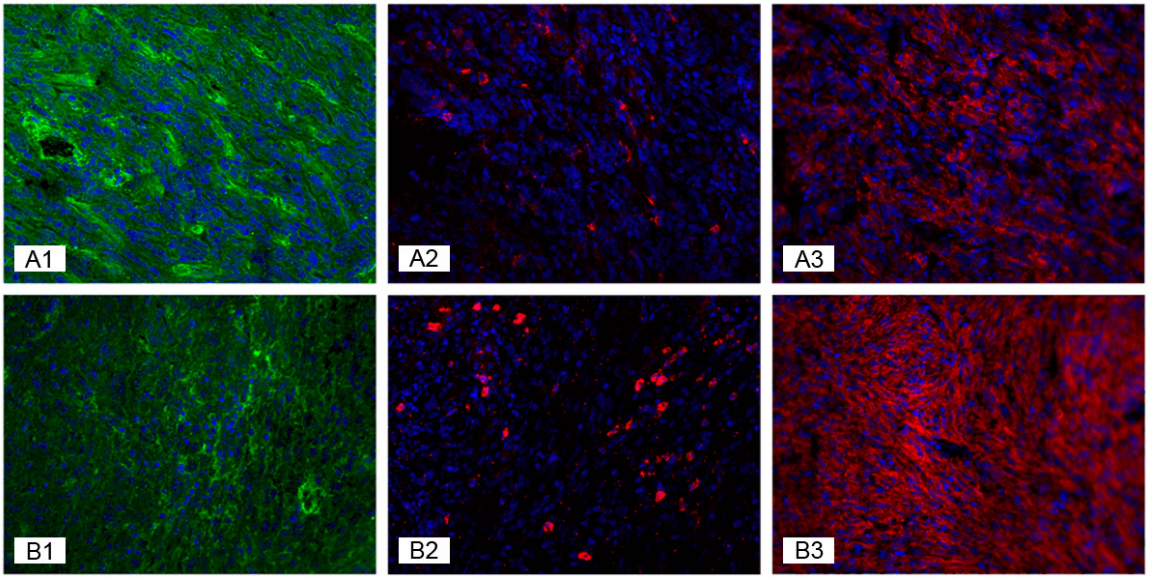

Figure 6. Immunofluorescent staining of kryosections of representative GISTs. (A) small intestinal GIST. (B) peritoneal metastasis. The horizontal photographs show immunostaining with anti-CXCL1 (green) (1), and its receptor CXCR2 (red) (2). For comparison anti-cKIT staining is depicted in (3). Anti-CXCL1 showed positivity in tumor cells and tumor vasculature. Its receptor, CXCR2 showed positivity in interstitial immune cells. Cell nuclear counterstaining was done with 4',-6-diamidino-2-phenylindole, visualized in blue. Scale bar 100 µm, original magnification ×200.

within the nucleus (**Figure 5**). CXCL1 was expressed by tumor cells, but was also positive in the tumor vasculature. Its receptor, CXCR2 showed positivity in interstitial, supposedly immune cells (**Figure 6**).

Discussion

Activating mutations in tyrosine kinase receptor genes are important for proliferation, cell cycle progression, and survival [57]. It thus remains unclear why micro-GIST, i.e. very small (0.2-10 mm) asymptomatic GIST, which contain receptor tyrosine kinase mutations, should not generally progress to malignancy [11, 58]. It has thus been hypothesized that they need additional stimuli to evolve into clinical GIST [11]. A tumor microenvironment seems essential for tumor progression. It is known that tumors are able to influence and maintain their own microenvironment, which includes immune cells, stromal cells and microvessels [59, 60]. Tumor-derived chemotactic factors drive the transmigration and immigration of host cells into the tumor. Secreted chemokines from various tumor cell lines have the ability to induce directional migration of i.e. monocytes [61, 62]. CCL2 is a major chemokine for this population [63]. And it has been shown, that monocytes can differentiate into tumor-associated macrophages (TAMs) and immature DCs [64].

The microenvironment of a metastasis might depend on its location and the surrounding tissue [65]. As for GIST, it has been shown that peritoneal metastasis is probably a consequence of primary tumor rupture or microscopic serosa penetration [66], whilst liver metastasis results from hematogenic spread. Interestingly, lymphatic spread can be neglected [67, 68].

In order to evaluate the differential immune cell infiltrate in primary GIST compared to liver and peritoneal metastases, we used a historical collective of 188 primary and 51 metastasized GIST without prior tyrosine-kinase inhibitor treatment, and quantitatively evaluated cells of the macrophage lineage (Ki-M1P, CD68) and cells of lymphoplasmacellular origin (CD3, CD20, CD56).

In primary as in all metastatic GIST, Ki-M1P+ cells were the predominant immune cells (28.8% ± 7.1, vs. 26.7% ± 6.3, respectively), pointing to their important role within the tumor microenvironment. They were significantly more common in epithelioid and mixed than in spindle-cellular GIST. Larger GIST (> 10 cm) and

GIST with a proliferation index > 10% had significantly more Ki-M1P+ cells. Their number was however not associated with risk of recurrence (after resection of the primary).

It is known, that tumor-associated macrophages secrete growth factors, promote angiogenesis and suppress antitumor functions of immune effector cells [30]. When comparing liver to peritoneal metastases, Ki-M1P+ cells were significantly more abundant in peritoneal metastases ($P < 0.01$). This might be due to the lack of structural tissue, surrounding peritoneal GIST metastases. The absence of cohesive tissue embedding a peritoneal metastasis might make stromal cells more relevant. The abundant number of Ki-M1P+ cells might even explain the higher proliferation rate of peritoneal metastases, when compared to liver metastases ($P < 0.05$). As GIST grow outwards without infiltration of the surrounding tissue, other mechanisms at the tumor front - than for instance in adenocarcinomas [69, 70] - might govern the tumor-host-relationship at its margins. Generation of regulatory T-cells upon encounter with M2 macrophages has been suggested as mechanism for local immune suppression [21, 71]. Accordingly, in GIST, analysis of the macrophage population showed a predominance of the M2-phenotype [21]. Also in our study, Ki-M1P+ mononuclear phagocytes were significantly more common than CD68+, generally lysosomal rich macrophages. It is known that tyrosine-kinase inhibitor treatment might influence the number and type of immune cells [18, 72, 73]. Imatinib has been shown to induce growth inhibition of monocytes/macrophages *in vitro*. This effect was attributed to down-regulation of the expression of macrophage colony-stimulating factor-1 receptor (CSF-1 or macrophage-CSF or c-fms) [74, 75].

Our current results in primary untreated GIST confirm our earlier findings that most lymphocytes were T-lymphocytes, as against a small number of CD20+ B-cells and CD56+ NK-cells [19]. Van Dongen et al. [21] showed that the balance of cytotoxic T-cells and Fox-P3 T-cells favored local immune suppression. Accordingly, we have already shown that gene expression of inflammatory cytokines in primary GIST is low, with TNF-α transcript expression being negligible [19]. Interestingly, compared to primary GIST, GIST metastases showed significantly more T-cells. This could mainly be attributed to the number of T-cells within the liver metastases compared to peritoneal metastases, which points to a different microenvironment at the different metastatic sites. As for tyrosine-kinase inhibitor treatment, it has been suggested that imatinib induces T-cell activation and apoptosis in GIST [18]. Even though such an alternate pathway of imatinib activity has not found its way into clinical treatment decisions, the idea of T-cell activation, as in melanoma [14], is intriguing. It is supported by anti-KIT designer T-cells which are able to produce IFNγ and lyse GIST cells in cell culture [33]. In a subcutaneous xenograft model, GIST cell growth could be inhibited by designer T-cells with IL-2 support [33]. It has further been shown that combination of imatinib with IL-2 activates NK cells, leading to tumor regression in animal models [73]. Rusakiewicz et al. [22] could show that after imatinib treatment, CD56+ NK cells accumulated in tumor foci.

A possible 'symbiotic relationship' between the GIST and its local immune cell infiltrate is further supported by our analysis of the chemokine profile within the tumor. The highest chemokine transcript expression in primary GIST was found for the CC-chemokine CCL2 (MCP1). CCL2 is associated with monocyte recruitment, transmigration and differentiation [40, 42, 76]. Within the tumor microenvironment, it might thus limit immunosurveillance and aid tumor growth [41, 77-79]. As for its location, our immunofluorescent analysis showed that CCL2 was expressed by tumor cells. CCL2 positivity was further found in endothelial cells within the tumor. Its receptor CCR2, showed staining of some tumor-infiltrating immune cells, but could especially be visualized within the tumor nuclei. It has been proposed that CCR2 expression in the nucleus might directly initiate or regulate transcriptional events [80]. In contrast to cell surface G-protein coupled receptors which mediate immediate effects, their nuclear location has been associated with initiation or regulation of transcriptional events and control of long-term responses [80, 81]. These might be important for tumor survival and progression [82-84]. In addition to the expression of CCL2, we found a high expression of CCL3 (MIP-1α) at transcript level. It has been suggested that expression of CCL3, not only by macrophages

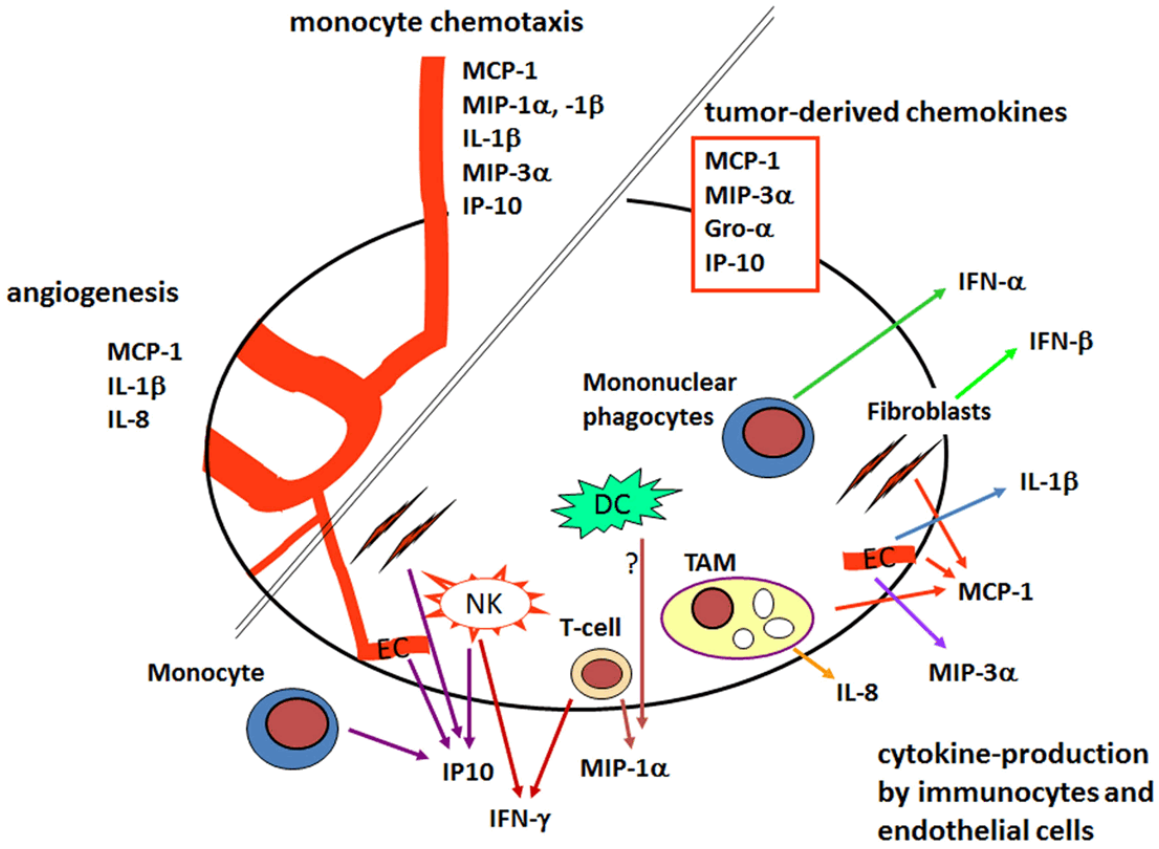

Figure 7. Schematic of the expression of cytokines and chemokines from tumors and their microenvironment, i.e. immune cells, fibroblasts and endothelial cells [12, 40-45, 76, 85, 88]. Arrows are depicted in color to highlight the expression of the various cytokines.

and fibroblasts but also by tumor tissue, points to an interaction between cancer cells and host immune cells [85], as suggested for CCL2 [79]. Even more than the aforementioned immune-cell attractant CC-chemokines, the growth-regulated oncogenes CXCL1-3 have been associated with tumor proliferation and metastatic potential [44, 45], as was Il-1β [86]). This effect is partly due to pro-angiogenic functions [12, 44, 45, 87]. Immunofluorescence visualization of CXCL1 confirmed its expression by tumor cells, but also showed positivity in the tumor vasculature. IL-8 transcript expression in our GIST cohort was for instance comparable to that of Il-1β described in our previous study [19]. Similar to other tumors, GIST might thus be able to control and maintain their own microenvironment (**Figure 7**). Accordingly, we could show previously that an inflammatory response against the tumor seems to be missing with negligible or low expression of the classic acute phase cytokines TNF-α and IL6 and low expression of interferons [19].

In conclusion, the different percentage of immune cells in primary GIST as well as peritoneal and liver metastases, points to a locally specific microenvironment which might influence neoplastic progression at the different sites. Ki-M1P+ cells seem to represent a special type of tumor-associated macrophages, with diverging expression within liver and peritoneal metastases. Further studies in view of chemokine expression of the primary and its metastases under treatment conditions would be helpful to understand tumor elimination by the therapy, equilibrium or tumor-escape to the local immune cell infiltrate.

Acknowledgements

We would like to thank Robert Cameron, Ph.D. (Max-Planck Institute for Solar System Research, Göttingen, Germany) for his contribution to the computer analysis programs. We thank the department of General, Visceral and Pediatric Surgery for their cooperation and pro-

vision of surgical specimen. We further thank Anke Herbst, Sonja Heyroth and Mercedes Martin-Ortega for their excellent technical assistance. We acknowledge support by Open Access Publication Funds of the University of Göttingen.

Disclosure of conflict of interest

None.

Address correspondence to: Dr. Silke Cameron, Clinic for Gastroenterology and Endocrinology, University Medicine Göttingen, Robert-Koch-Strasse 40, D-37075 Göttingen, Germany. Tel: +49-(0)551/39-6391; Fax: +49-(0)551/39-6921; E-mail: silke.cameron@med.uni-goettingen.de

References

[1] Miettinen M and Lasota J. Gastrointestinal stromal tumors: pathology and prognosis at different sites. Semin Diagn Pathol 2006; 23: 70-83.

[2] Heinrich MC, Rubin BP, Longley BJ and Fletcher JA. Biology and genetic aspects of gastrointestinal stromal tumors: KIT activation and cytogenetic alterations. Hum Pathol 2002; 33: 484-495.

[3] Miettinen M and Lasota J. Gastrointestinal stromal tumors (GISTs): definition, occurrence, pathology, differential diagnosis and molecular genetics. Pol J Pathol 2003; 54: 3-24.

[4] Miettinen M, Sobin LH and Lasota J. Gastrointestinal stromal tumors of the stomach: a clinicopathologic, immunohistochemical, and molecular genetic study of 1765 cases with long-term follow-up. Am J Surg Pathol 2005; 29: 52-68.

[5] Miettinen M and Lasota J. Gastrointestinal stromal tumors: pathology and prognosis at different sites. Semin Diagn Pathol 2006; 23: 70-83.

[6] Hohenberger P and Wardelmann E. [Surgical considerations for gastrointestinal stroma tumor]. Chirurg 2006; 77: 33-40.

[7] Sobin L, Gospodarowicz M and Wittekind C. TNM Classification of Malignant Tumours. 2009.

[8] Fletcher CD, Berman JJ, Corless C, Gorstein F, Lasota J, Longley BJ, Miettinen M, O'Leary TJ, Remotti H, Rubin BP, Shmookler B, Sobin LH and Weiss SW. Diagnosis of gastrointestinal stromal tumors: A consensus approach. Hum Pathol 2002; 33: 459-465.

[9] Agaimy A, Otto C, Braun A, Geddert H, Schaefer IM and Haller F. Value of epithelioid morphology and PDGFRA immunostaining pattern for prediction of PDGFRA mutated genotype in gastrointestinal stromal tumors (GISTs). Int J Clin Exp Pathol 2013; 6: 1839-1846.

[10] Haller F, Cortis J, Helfrich J, Cameron S, Schuler P, Schwager S, Gunawan B, Fuzesi L and Agaimy A. Epithelioid/mixed phenotype in gastrointestinal stromal tumors with KIT mutation from the stomach is associated with accelerated passage of late phases of the cell cycle and shorter disease-free survival. Mod Pathol 2011; 24: 248-255.

[11] Agaimy A, Wunsch PH, Hofstaedter F, Blaszyk H, Rummele P, Gaumann A, Dietmaier W and Hartmann A. Minute gastric sclerosing stromal tumors (GIST tumorlets) are common in adults and frequently show c-KIT mutations. Am J Surg Pathol 2007; 31: 113-120.

[12] Lattanzio L, Tonissi F, Torta I, Gianello L, Russi E, Milano G, Merlano M and Lo NC. Role of IL-8 induced angiogenesis in uveal melanoma. Invest New Drugs 2013; 31: 1107-1114.

[13] Neesse A, Michl P, Frese KK, Feig C, Cook N, Jacobetz MA, Lolkema MP, Buchholz M, Olive KP, Gress TM and Tuveson DA. Stromal biology and therapy in pancreatic cancer. Gut 2011; 60: 861-868.

[14] Tsaknakis B, Schaefer IM, Schworer H, Sahlmann CO, Thoms KM, Blaschke M, Ramadori G and Cameron S. Long-lasting complete response of metastatic melanoma to ipilimumab with analysis of the resident immune cells. Med Oncol 2014; 31: 813

[15] Coussens LM and Werb Z. Inflammation and cancer. Nature 2002; 420: 860-867.

[16] Galon J, Costes A, Sanchez-Cabo F, Kirilovsky A, Mlecnik B, Lagorce-Pages C, Tosolini M, Camus M, Berger A, Wind P, Zinzindohoue F, Bruneval P, Cugnenc PH, Trajanoski Z, Fridman WH and Pages F. Type, density, and location of immune cells within human colorectal tumors predict clinical outcome. Science 2006; 313: 1960-1964.

[17] Tlsty TD and Coussens LM. Tumor stroma and regulation of cancer development. Annu Rev Pathol 2006; 1: 119-150.

[18] Balachandran VP, Cavnar MJ, Zeng S, Bamboat ZM, Ocuin LM, Obaid H, Sorenson EC, Popow R, Ariyan C, Rossi F, Besmer P, Guo T, Antonescu CR, Taguchi T, Yuan J, Wolchok JD, Allison JP and DeMatteo RP. Imatinib potentiates antitumor T cell responses in gastrointestinal stromal tumor through the inhibition of Ido. Nat Med 2011; 17: 1094-1100.

[19] Cameron S, Haller F, Dudas J, Moriconi F, Gunawan B, Armbrust T, Langer C, Fuzesi L and Ramadori G. Immune cells in primary gastrointestinal stromal tumors. Eur J Gastroenterol Hepatol 2008; 20: 327-334.

[20] Menard C, Blay JY, Borg C, Michiels S, Ghiringhelli F, Robert C, Nonn C, Chaput N, Taieb J, Delahaye NF, Flament C, Emile JF, Le CA and Zitvogel L. Natural killer cell IFN-gamma levels predict long-term survival with imatinib mesylate therapy in gastrointestinal stromal tumor-bearing patients. Cancer Res 2009; 69: 3563-3569.

[21] van Dongen M, Savage ND, Jordanova ES, Briaire-de Bruijn IH, Walburg KV, Ottenhoff TH, Hogendoorn PC, van der Burg SH, Gelderblom H and van HT. Anti-inflammatory M2 type macrophages characterize metastasized and tyrosine kinase inhibitor-treated gastrointestinal stromal tumors. Int J Cancer 2010; 127: 899-909.

[22] Rusakiewicz S, Semeraro M, Sarabi M, Desbois M, Locher C, Mendez R, Vimond N, Concha A, Garrido F, Isambert N, Chaigneau L, Le Brun-Ly V, Dubreuil P, Cremer I, Caignard A, Poirier-Colame V, Chaba K, Flament C, Halama N, Jager D, Eggermont A, Bonvalot S, Commo F, Terrier P, Opolon P, Emile JF, Coindre JM, Kroemer G, Chaput N, Le CA, Blay JY and Zitvogel L. Immune infiltrates are prognostic factors in localized gastrointestinal stromal tumors. Cancer Res 2013; 73: 3499-3510.

[23] Dvorak HF. Tumors: wounds that do not heal. Similarities between tumor stroma generation and wound healing. N Engl J Med 1986; 315: 1650-1659.

[24] Vendramini-Costa DB and Carvalho JE. Molecular link mechanisms between inflammation and cancer. Curr Pharm Des 2012; 18: 3831-3852.

[25] Gu M, Ghafari S, Nguyen PT, and Lin F. Cytologic diagnosis of gastrointestinal stromal tumors of the stomach by endoscopic ultrasound-guided fine-needle aspiration biopsy: cytomorphologic and immunohistochemical study of 12 cases. Diagn Cytopathol 2001; 25: 343-350.

[26] Rogler G. Chronic ulcerative colitis and colorectal cancer. Cancer Lett 2013.

[27] Thanan R, Pairojkul C, Pinlaor S, Khuntikeo N, Wongkham C, Sripa B, Ma N, Vaeteewoottacharn K, Furukawa A, Kobayashi H, Hiraku Y, Oikawa S, Kawanishi S, Yongvanit P and Murata M. Inflammation-related DNA damage and expression of CD133 and Oct3/4 in cholangiocarcinoma patients with poor prognosis. Free Radic Biol Med 2013; 65: 1464-72.

[28] Hussein MR. Dendritic cells and melanoma tumorigenesis: an insight. Cancer Biol Ther 2005; 4: 501-505.

[29] Vermi W, Bonecchi R, Facchetti F, Bianchi D, Sozzani S, Festa S, Berenzi A, Cella M and Colonna M. Recruitment of immature plasmacytoid dendritic cells (plasmacytoid monocytes) and myeloid dendritic cells in primary cutaneous melanomas. J Pathol 2003; 200: 255-268.

[30] Lewis CE and Pollard JW. Distinct role of macrophages in different tumor microenvironments. Cancer Res 2006; 66: 605-612.

[31] Mantovani A, Sica A, Sozzani S, Allavena P, Vecchi A and Locati M. The chemokine system in diverse forms of macrophage activation and polarization. Trends Immunol 2004; 25: 677-686.

[32] Hamid O, Schmidt H, Nissan A, Ridolfi L, Aamdal S, Hansson J, Guida M, Hyams DM, Gomez H, Bastholt L, Chasalow SD and Berman D. A prospective phase II trial exploring the association between tumor microenvironment biomarkers and clinical activity of ipilimumab in advanced melanoma. J Transl Med 2011; 9: 204

[33] Katz SC, Burga RA, Naheed S, Licata LA, Thorn M, Osgood D, Nguyen CT, Espat NJ, Fletcher JA and Junghans RP. Anti-KIT designer T cells for the treatment of gastrointestinal stromal tumor. J Transl Med 2013; 11: 46

[34] Quezada SA, Peggs KS, Curran MA and Allison JP. CTLA4 blockade and GM-CSF combination immunotherapy alters the intratumor balance of effector and regulatory T cells. J Clin Invest 2006; 116: 1935-1945.

[35] Smyth MJ. Imatinib mesylate–uncovering a fast track to adaptive immunity. N Engl J Med 2006; 354: 2282-2284.

[36] Taieb J, Chaput N, Menard C, Apetoh L, Ullrich E, Bonmort M, Pequignot M, Casares N, Terme M, Flament C, Opolon P, Lecluse Y, Metivier D, Tomasello E, Vivier E, Ghiringhelli F, Martin F, Klatzmann D, Poynard T, Tursz T, Raposo G, Yagita H, Ryffel B, Kroemer G and Zitvogel L. A novel dendritic cell subset involved in tumor immunosurveillance. Nat Med 2006; 12: 214-219.

[37] Graeme-Cook F, Bhan AK and Harris NL. Immunohistochemical characterization of intraepithelial and subepithelial mononuclear cells of the upper airways. Am J Pathol 1993; 143: 1416-1422.

[38] Radzun HJ, Hansmann ML, Heidebrecht HJ, Bodewadt-Radzun S, Wacker HH, Kreipe H, Lumbeck H, Hernandez C, Kuhn C and Parwaresch MR. Detection of a monocyte/macrophage differentiation antigen in routinely processed paraffin-embedded tissues by monoclonal antibody Ki-M1P. Lab Invest 1991; 65: 306-315.

[39] Goyert SM. CD68 workshop panel report. Leukocyte Typing VI White Cell Differentiation Antigens Proceedings of the 6th International Workshop and Conference 1996 1997; 1359-1372.

[40] Gerszten RE, Garcia-Zepeda EA, Lim YC, Yoshida M, Ding HA, Gimbrone MA Jr, Luster AD, Luscinskas FW and Rosenzweig A. MCP-1 and IL-8 trigger firm adhesion of monocytes to vascular endothelium under flow conditions. Nature 1999; 398: 718-723.

[41] Kuroda T, Kitadai Y, Tanaka S, Yang X, Mukaida N, Yoshihara M and Chayama K. Monocyte chemoattractant protein-1 transfection induces angiogenesis and tumorigenesis of gastric carcinoma in nude mice via macrophage recruitment. Clin Cancer Res 2005; 11: 7629-7636.

[42] Weber KS, von HP, Clark-Lewis I, Weber PC and Weber C. Differential immobilization and hierarchical involvement of chemokines in monocyte arrest and transmigration on inflamed endothelium in shear flow. Eur J Immunol 1999; 29: 700-712.

[43] Haghnegahdar H, Du J, Wang D, Strieter RM, Burdick MD, Nanney LB, Cardwell N, Luan J, Shattuck-Brandt R and Richmond A. The tumorigenic and angiogenic effects of MGSA/GRO proteins in melanoma. J Leukoc Biol 2000; 67: 53-62.

[44] Li A, Varney ML and Singh RK. Constitutive expression of growth regulated oncogene (gro) in human colon carcinoma cells with different metastatic potential and its role in regulating their metastatic phenotype. Clin Exp Metastasis 2004; 21: 571-579.

[45] Zhou Y, Zhang J, Liu Q, Bell R, Muruve DA, Forsyth P, Arcellana-Panlilio M, Robbins S and Yong VW. The chemokine GRO-alpha (CXCL1) confers increased tumorigenicity to glioma cells. Carcinogenesis 2005; 26: 2058-2068.

[46] Flesch IE, Barsig J and Kaufmann SH. Differential chemokine response of murine macrophages stimulated with cytokines and infected with Listeria monocytogenes. Int Immunol 1998; 10: 757-765.

[47] Maurer M and von SE. Macrophage inflammatory protein-1. Int J Biochem Cell Biol 2004; 36: 1882-1886.

[48] Tanaka Y, Adams DH, Hubscher S, Hirano H, Siebenlist U and Shaw S. T-cell adhesion induced by proteoglycan-immobilized cytokine MIP-1 beta. Nature 1993; 361: 79-82.

[49] Miettinen M, El-Rifai W, Sobin HL and Lasota J. Evaluation of malignancy and prognosis of gastrointestinal stromal tumors: a review. 2002; 33: 478-483.

[50] Mason DY, Cordell J, Brown M, Pallesen G, Ralfkiaer E, Rothbard J, Crumpton M and Gatter KC. Detection of T cells in paraffin wax embedded tissue using antibodies against a peptide sequence from the CD3 antigen. J Clin Pathol 1989; 42: 1194-1200.

[51] Tedder TF and Engel P. CD20: a regulator of cell-cycle progression of B lymphocytes. Immunol Today 1994; 15: 450-454.

[52] Borg C, Terme M, Taieb J, Menard C, Flament C, Robert C, Maruyama K, Wakasugi H, Angevin E, Thielemans K, Le CA, Chung-Scott V, Lazar V, Tchou I, Crepineau F, Lemoine F, Bernard J, Fletcher JA, Turhan A, Blay JY, Spatz A, Emile JF, Heinrich MC, Mecheri S, Tursz T and Zitvogel L. Novel mode of action of c-kit tyrosine kinase inhibitors leading to NK cell-dependent antitumor effects. J Clin Invest 2004; 114: 379-388.

[53] Dalbeth N, Gundle R, Davies RJ, Lee YC, McMichael AJ and Callan MF. CD56bright NK cells are enriched at inflammatory sites and can engage with monocytes in a reciprocal program of activation. J Immunol 2004; 173: 6418-6426.

[54] Haller F, Lobke C, Ruschhaupt M, Cameron S, Schulten HJ, Schwager S, von HA, Gunawan B, Langer C, Ramadori G, Sultmann H, Poustka A, Korf U and Fuzesi L. Loss of 9p leads to p16INK4A down-regulation and enables RB/E2F1-dependent cell cycle promotion in gastrointestinal stromal tumours (GISTs). J Pathol 2008; 215: 253-262.

[55] Haller F, Gunawan B, von HA, Schwager S, Schulten HJ, Wolf-Salgo J, Langer C, Ramadori G, Sultmann H and Fuzesi L. Prognostic role of E2F1 and members of the CDKN2A network in gastrointestinal stromal tumors. Clin Cancer Res 2005; 11: 6589-6597.

[56] Pfaffl MW. A new mathematical model for relative quantification in real-time RT-PCR. Nucleic Acids Res 2001; 29: e45

[57] Zwick E, Bange J and Ullrich A. Receptor tyrosine kinases as targets for anticancer drugs. Trends Mol Med 2002; 8: 17-23.

[58] Kawanowa K, Sakuma Y, Sakurai S, Hishima T, Iwasaki Y, Saito K, Hosoya Y, Nakajima T and Funata N. High incidence of microscopic gastrointestinal stromal tumors in the stomach. Hum Pathol 2006; 37: 1527-1535.

[59] Khan S, Cameron S, Blaschke M, Moriconi F, Naz N, Amanzada A, Ramadori G and Malik IA. Differential gene expression of chemokines in KRAS and BRAF mutated colorectal cell lines: role of cytokines. World J Gastroenterol 2014; 20: 2979-2994.

[60] Wang JM, Deng X, Gong W and Su S. Chemokines and their role in tumor growth and metastasis. J Immunol Methods 1998; 220: 1-17.

[61] Bottazzi B, Polentarutti N, Acero R, Balsari A, Boraschi D, Ghezzi P, Salmona M and Mantovani A. Regulation of the macrophage content of neoplasms by chemoattractants. Science 1983; 220: 210-212.

[62] Mantovani A. Tumor-associated macrophages in neoplastic progression: a paradigm for the in vivo function of chemokines. Lab Invest 1994; 71: 5-16.
[63] Deshmane SL, Kremlev S, Amini S and Sawaya BE. Monocyte chemoattractant protein-1 (MCP-1): an overview. J Interferon Cytokine Res 2009; 29: 313-326.
[64] Kim R, Emi M, Tanabe K and Arihiro K. Tumor-driven evolution of immunosuppressive networks during malignant progression. Cancer Res 2006; 66: 5527-5536.
[65] Vidal-Vanaclocha F. The prometastatic microenvironment of the liver. Cancer Microenviron 2008; 1: 113-129.
[66] Agaimy A, Vassos N, Wunsch PH, Hohenberger W, Hartmann A and Croner RS. Impact of serosal involvement/extramural growth on the risk of synchronous and metachronous peritoneal spread in gastrointestinal stromal tumors: proposal for a macroscopic classification of GIST. Int J Clin Exp Pathol 2012; 5: 12-22.
[67] Beham AW, Schaefer IM, Schuler P, Cameron S and Ghadimi BM. Gastrointestinal stromal tumors. Int J Colorectal Dis 2012; 27: 689-700.
[68] Gold JS and DeMatteo RP. Combined surgical and molecular therapy: the gastrointestinal stromal tumor model. Ann Surg 2006; 244: 176-184.
[69] Bandapalli OR, Dihlmann S, Helwa R, Macher-Goeppinger S, Weitz J, Schirmacher P and Brand K. Transcriptional activation of the beta-catenin gene at the invasion front of colorectal liver metastases. J Pathol 2009; 218: 370-379.
[70] Kahlert C, Bandapalli OR, Schirmacher P, Weitz J and Brand K. Invasion front-specific overexpression of tissue inhibitor of metalloproteinase-1 in liver metastases from colorectal cancer. Anticancer Res 2008; 28: 1459-1465.
[71] Savage ND, de BT, Walburg KV, Joosten SA, van MK, Geluk A and Ottenhoff TH. Human anti-inflammatory macrophages induce Foxp3+ GITR+ CD25+ regulatory T cells, which suppress via membrane-bound TGFbeta-1. J Immunol 2008; 181: 2220-2226.
[72] Perez DR, Baser RE, Cavnar MJ, Balachandran VP, Antonescu CR, Tap WD, Strong VE, Brennan MF, Coit DG, Singer S and DeMatteo RP. Blood neutrophil-to-lymphocyte ratio is prognostic in gastrointestinal stromal tumor. Ann Surg Oncol 2013; 20: 593-599.
[73] Wolf D, Tilg H, Rumpold H, Gastl G and Wolf AM. The kinase inhibitor imatinib--an immunosuppressive drug? Curr Cancer Drug Targets 2007; 7: 251-258.
[74] Dewar AL, Cambareri AC, Zannettino AC, Miller BL, Doherty KV, Hughes TP and Lyons AB. Macrophage colony-stimulating factor receptor c-fms is a novel target of imatinib. Blood 2005; 105: 3127-3132.
[75] Taylor JR, Brownlow N, Domin J and Dibb NJ. FMS receptor for M-CSF (CSF-1) is sensitive to the kinase inhibitor imatinib and mutation of Asp-802 to Val confers resistance. Oncogene 2006; 25: 147-151.
[76] Omata N, Yasutomi M, Yamada A, Iwasaki H, Mayumi M and Ohshima Y. Monocyte chemoattractant protein-1 selectively inhibits the acquisition of CD40 ligand-dependent IL-12-producing capacity of monocyte-derived dendritic cells and modulates Th1 immune response. J Immunol 2002; 169: 4861-4866.
[77] Mizutani K, Sud S, McGregor NA, Martinovski G, Rice BT, Craig MJ, Varsos ZS, Roca H and Pienta KJ. The chemokine CCL2 increases prostate tumor growth and bone metastasis through macrophage and osteoclast recruitment. Neoplasia 2009; 11: 1235-1242.
[78] Saji H, Koike M, Yamori T, Saji S, Seiki M, Matsushima K and Toi M. Significant correlation of monocyte chemoattractant protein-1 expression with neovascularization and progression of breast carcinoma. Cancer 2001; 92: 1085-1091.
[79] Li M, Knight DA, Snyder A, Smyth MJ and Stewart TJ. A role for CCL2 in both tumor progression and immunosurveillance. Oncoimmunology 2013; 2: e25474
[80] Favre N, Camps M, Arod C, Chabert C, Rommel C and Pasquali C. Chemokine receptor CCR2 undergoes transportin1-dependent nuclear translocation. Proteomics 2008; 8: 4560-4576.
[81] Goetzl EJ. Diverse pathways for nuclear signaling by G protein-coupled receptors and their ligands. FASEB J 2007; 21: 638-642.
[82] Liang Y, Bollen AW and Gupta N. CC chemokine receptor-2A is frequently overexpressed in glioblastoma. J Neurooncol 2008; 86: 153-163.
[83] Lu Y, Cai Z, Xiao G, Liu Y, Keller ET, Yao Z and Zhang J. CCR2 expression correlates with prostate cancer progression. J Cell Biochem 2007; 101: 676-685.
[84] Van de BI, Leleu X, Schots R, Facon T, Vanderkerken K, Van CB and Van RI. Clinical significance of chemokine receptor (CCR1, CCR2 and CXCR4) expression in human myeloma cells: the association with disease activity and survival. Haematologica 2006; 91: 200-206.
[85] Konishi T, Okabe H, Katoh H, Fujiyama Y and Mori A. Macrophage inflammatory protein-1 alpha expression in non-neoplastic and neoplastic lung tissue. Virchows Arch 1996; 428: 107-111.
[86] Saijo Y, Tanaka M, Miki M, Usui K, Suzuki T, Maemondo M, Hong X, Tazawa R, Kikuchi T,

Matsushima K and Nukiwa T. Proinflammatory cytokine IL-1 beta promotes tumor growth of Lewis lung carcinoma by induction of angiogenic factors: in vivo analysis of tumor-stromal interaction. J Immunol 2002; 169: 469-475.

[87] Xu J, Yin Z, Cao S, Gao W, Liu L, Yin Y, Liu P and Shu Y. Systematic review and meta-analysis on the association between IL-1B polymorphisms and cancer risk. PLoS One 2013; 8: e63654

[88] Heidemann J, Ogawa H, Dwinell MB, Rafiee P, Maaser C, Gockel HR, Otterson MF, Ota DM, Lugering N, Domschke W and Binion DG. Angiogenic effects of interleukin 8 (CXCL8) in human intestinal microvascular endothelial cells are mediated by CXCR2. J Biol Chem 2003; 278: 8508-8515.